Solar seasonal thermal energy storage for space heating in residential buildings: Optimization and comparison with an air-source heat pump

Jie Lu , Guoqing He & Feng Mao

Taylor & Francis
Taylor & Francis Group

Check for updates

Solar seasonal thermal energy storage for space heating in residential buildings: Optimization and comparison with an air-source heat pump

Jie Lu[a], Guoqing He [a], and Feng Mao[b]

[a]College of Civil Engineering and Architecture, Zhejiang University, Hangzhou, China; [b]Department of Marketing, Hangzhou Huadian Huayuan Environment Engineering Co.,Ltd, Hangzhou, China

ABSTRACT

This study evaluates the techno-economics of replacing an air-source heat pump (ASHP) system with a solar seasonal thermal energy storage (STES) system for space heating in Hangzhou, China. Three heating systems, solar STES, ASHP, and ASHP with short-term storage of solar energy, are developed using TRNSYS for a house with 240 m^2 of floor area. The ratio of tank volume to collector area (RVA) of the STES is optimized for the lowest equivalent annual cost over a lifespan of 20 y. The determined optimal RVA is 0.33 m^3/m^2, although it depends on the system and electricity prices. The optimized STES reduces the electricity demand to 1,269 kWh (74% reduction). Despite the superior energy performance, the economic benefit is only possible with large STES systems, which enjoy low tank prices due to scale effects. The results suggest that policy support is needed for STES, where district scaling is not an option.

1. Introduction

Solar thermal utilization is a technically mature renewable solution for the supply of domestic hot water in the global effort to reduce fossil fuel consumption (Hepbasli, Ulgen, and Eke 2004; Hovsepian and Kaiser 1997). Despite the significant growth in installations over the past couple of decades, the penetration of solar thermal systems still faces substantial economic and social barriers (Hang, Qu, and Zhao 2012; Leckner and Zmeureanu 2011; Martinopoulos and Tsalikis 2018; Sovacool and Martiskainen 2020; Urmeea et al. 2018). Among these barriers is the lower cost of electricity (Azeez and Atikol 2019). Recently, the use of solar thermal energy in space heating has been attracting attention (Huang, Fan, and Furbo 2019; Marcos, Izquierdo, and Parra 2011; Martinopoulos and Tsalikis 2014), especially in northern Europe, where district heating is increasing and seasonal energy storage technology has been developed to improve the energy performance of solar thermal systems (Dahash et al. 2019).

In the hot summer cold winter (HSCW) region of China, domestic space heating is a fast-growing market (Zhang, Zheng, and Huang 2014), and solar energy is considered an appealing alternative to cope with air pollution and energy pressure (Huang and Huang 2017). Local governments have planned to increase the share of renewable energy in the heating market (Huang, Fan, and Furbo 2019). Incentive policies and regulations have been made to promote building designs that incorporate solar energy and heat pumps (He et al. 2015).

Solar energy would be an ideal heating energy source except for two issues: 1) It is least abundant in winter when it is needed most. 2) Its energy density is low, and substantial investment in solar

---

This article has been republished with minor changes. These changes do not impact the academic content of the article.

collectors is required. Seasonal thermal energy storage (STES) systems appear to be a promising solution to these issues by storing excessive summer solar energy in rocks, soil, aquifers, or water tanks for use in winter (Dahash et al. 2019; Hesaraki, Halilovic, and Holmberg 2015). To date, many sizable central heating systems have been constructed, mostly in Europe (Bokhoven and Van Dam 2001; Jradi, Veje, and Jørgensen 2017; Ochs, Heidemann, and Müller-Steinhagen 2009; Paksoy et al. 2000) and in other countries as well (Chung, Park, and Yoon 1998; Krupczak et al. 1986; Li et al. 2015; Walton and McSwiggen 1983; Zhang et al. 2015). Most STES projects store energy in the form of sensible heat (mostly water), while latent heat and chemical methods are considered promising but are not yet mature (Fatih Demirbas 2006; Xu and Wang 2019). In cold climates, the borehole system assisted with a heat pump is recommended (Shah, Aye, and Rismanchi 2018). However, due to the high water table level in HSCW regions, STES systems with a water tank or pit are probably a more suitable choice. Therefore, this study focuses on tank STES systems.

For tank systems, the initial investment is dependent mainly on the size of the tank and solar collectors. Their proper sizing is critical not only for energy capacity but also for economic performance (McKenna, Fehrenbach, and Merkel 2019). In the literature, the ratio of the storage volume to the collector area (RVA, m^3/m^2) has received much attention. Much discussion of this value has been energy-oriented with a special focus on the energy efficiency or energy capacity of the storage system, leading to relatively large storage systems. Guadalfajara et al. (2015) proposed an RVA value of 6.1 m^3/m^2 to ensure no rejection of collected solar energy. In other studies (Durão, Joyce, and Mendes 2014; Hesaraki, Halilovic, and Holmberg 2015), a similar ratio (5 m^3/m^2) was recommended for maximum efficiency. From the review work by Dahash et al. (2019), most large-scale district heating projects constructed in Germany, Denmark, and several other European countries in the last two decades have a ratio greater than 1 m^3/m^2 and some as high as 5.6 m^3/m^2. Smaller RVA values, however, also have been suggested for domestic heating systems. Li et al. (2014) proposed that a storage factor of 0.567 m^3/m^2 was most suitable for a system in Beijing considering the balance between storage efficiency and solar collector efficiency. Ma et al. (2018) calculated the preferred RVA as ranging from 0.67 to 1.0 m^3/m^2 for residential houses in the UK, assuming that the STES system met 100% of the heating demand. Beausoleil-Morrison et al. (2019) recommended a 36 m^3 tank and a 41.6 m^2 collector (RVA = 0.87 m^3/m^2) for a residential project.

However, all RVA values from projects adopting seasonal storage are still an order of magnitude higher than those without considering seasonal storage (Hang, Qu, and Zhao 2012; Li et al. 2015; Marcos, Izquierdo, and Parra 2011). For example, for a tank of 0.3 m^3, Leckner and Zmeureanu (2011) found that a collector area of 11 m^2 was best to maximize the energy reduction for a house in Canada. In Greece, Martinopoulos and Tsalikis (2014) suggested that from an economic point of view, 12 m^2 of collectors with a tank of 0.5 or 0.65 m^3 is the best combination for energy-efficient houses in four cities.

Thus far, to the best of our knowledge, few studies have discussed the optimization of the STES RVA based on economic performance. Launay et al. (2019) presented an optimal analysis of a residential project using multiple criteria, including solar fraction and the Levelized Cost of energy; however, they did not provide an optimized sizing for the minimum Levelized Cost of the energy. Although STES projects may still need policy support (Milewski, Wołowicz, and Bujalski 2013; Renaldi and Friedrich 2019), the economic aspect of STES is an essential factor in the decision-making process. The economic performance will depend on climate, geological conditions, local market conditions, and policies. Unlike most studies in the literature where the cost-effectiveness of the STES is evaluated against conventional energy sources, such as natural gas or electricity, this study analyzes the cost-effectiveness of the STES system through comparison with the popular ASHP heating system, which is accepted as an energy-efficient system (Li et al. 2007; Liu et al. 2016) in the HSCW region. The objective is to evaluate the economic feasibility of replacing the ASHP with a solar STES to reduce the growing rate of electricity demand in the heating market. The results will help policymakers and designers to incorporate the best of this technology in this region.

2. Methodology

The scope of the problem is to provide space heating for residential buildings in Hangzhou city in the HSCW region using as much solar energy as possible with economic performance as a constraint.

2.1. Building and site

Hangzhou city (30°16′N, 120°12′E) lies in the lower basin of the Yangtze River. Its climate produces a strong demand for both cooling (summer) and heating (winter). Based on the Typical Meteorological Year data provided by the China Meteorological Administration and Tsinghua University (2005), the daily average temperature varies between – 5°C and 37°C and the average total horizontal solar irradiation is 13.5 MJ/(m²·day). The variations of the solar radiation and ambient temperature are plotted in Figure 6(a,b), respectively. In this study, a heating period of 120 days (2880 h) from November 15 to March 15 of the next year was considered.

The heating demand of an energy-efficient two-story house with 240 m² floor area was used. It is a 12 m wide and 10 m long rectangular-shaped building with a tilted rooftop for solar collector installation. Note that the building model represents a low-energy building with a well-insulated envelope. The dynamic heating demand was simulated using the TRNSYS software (Klein and Beckman 2004) at a time step of 15 min. The weather data file was imported as an external file in Type 109 data reader in the standard TMY2 format. The building thermal load was modeled either using the Type 12 c model if the floor heating system was used or the Type 88 model if fan coil units were used. The Type 14 c component was selected to account for the internal gains from the occupants, appliances, and lighting equipment. The calculated total heating demand is 11,361 kWh (or 48 kWh/m²), and the maximum heating power is 25 kW. In terms of heating demand per floor area, the house just meets the building energy efficiency standard of 65% target of the leading cities in Northern China and the German WSVO'1995 standard (Zhou et al. 2018).

2.2. Systems and simulation

Three heating systems were designed and compared: the ASHP heating system, ASHP with solar water heating (SWH) as the auxiliary heating source (ASHP + SWH), and STES + SWH system using electrical heating as the auxiliary heating source. The water-source heat pump (WSHP) was used to assist the STES+SWH system.

2.2.1. System A: STES+SWH system
System A is a STES+SWH system with WSHP working in series (Figure 1). The solar collector charges the STES system all year long, which provides heat to the house during the heating period either directly or via the WSHP.

A model representation in TRNSYS is illustrated in Figure 2. The system consists of three subsystems, namely the solar collecting system, the storage system, and the floor heating system. The solar collecting system consists of solar collectors (Type 1b), a circulating pump (Type 3), and a controller (Type 2b) that manages the circulation of water between the collector and the storage tank. The controller initiates circulation once the temperature at the outlet of the collectors exceeds the temperature at the bottom of the tank by a set difference value and switches off the pump if the exceedance is below another set difference value. Moreover, the controller continually monitors the top node temperature of the tank for safety purposes and stops charging the tank once its temperature reaches 95°C.

The seasonal storage tank is a buried, orthogonal-shaped-stratified tank (Type 534). To model the stratified tank in TRNSYS, a previous study used five nodes to address the vertical temperature change (Antoniadis and Martinopoulos 2019). In our study, eight nodes were
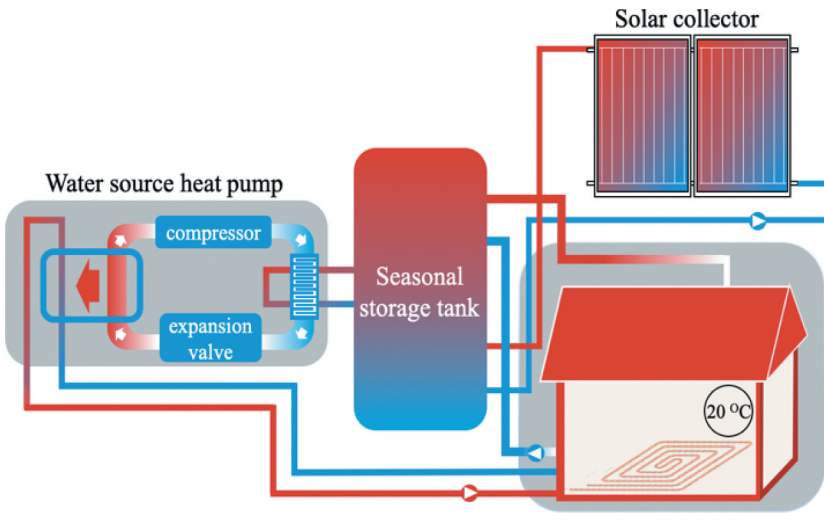
Figure 1. System A: seasonal thermal energy storage (STES) + solar water heating (SWH) with a floor heating system.
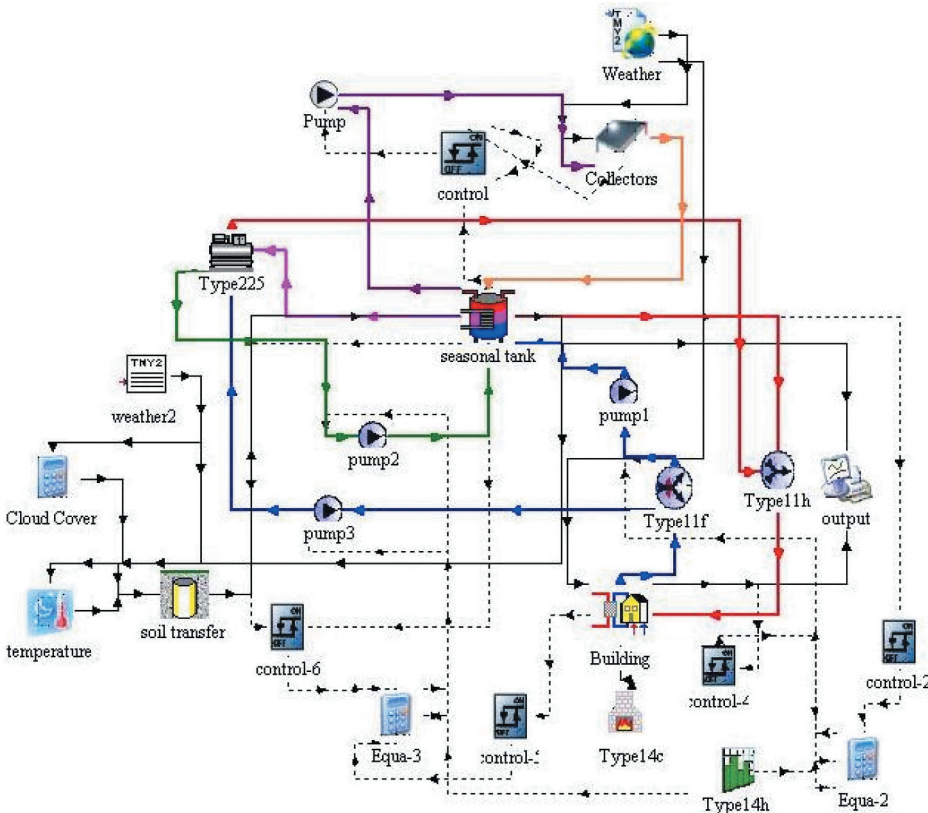

Figure 2. Modeling of the seasonal thermal energy storage (STES)+solar water heating (SWH) system in TRNSYS.

used as a result of balancing between accuracy and simulation speed. The size was determined such that the STES + WSHP system can meet 100% of the heating demand. The heat exchange between layers is processed through mass flow and free convection. Thermal

charging from the solar loop is realized through direct water exchange. The tank has an average heat loss rate of 0.333 W/(m²·K) to the surrounding soil. Soil temperature is a critical parameter in the estimation of the thermal loss of the tank. This parameter is, however, often not available, for which some simple methods have been used in the literature. For example, Sweet and McLeskey (2012) used a yearly constant temperature of the soil, while Hesaraki et al. (2015) used the mean annual outdoor temperature as the ground temperature. In this study, the heat transfer between the tank and environment was simulated using the Type 707 object in TRNSYS with the dynamic temperature of the soil according to the weather data of Hangzhou (Zhang, Wang, and Fu 2006).

The floor heating system was used such that a relatively low water supply temperature could be used to match the SWH or heat pump heating systems. The Type 12 c was used to simulate the building with floor heating systems for its excellent representation of the building heating load and less calculation time (Antoniadis and Martinopoulos 2019). During the heating period, the STES provides hot water directly to the building for space heating if the water temperature is above 40°C. Otherwise, the water temperature is raised through the WSHP. Electrical heating would serve the same purpose in terms of energy efficiency; however, the heat pump has a much larger heating capacity for the same-rated power. A variable-speed compressor ensures that the supply water temperature can be adjusted to match the heating demand. The heat pump has a nominal coefficient of performance (COP) of 4. The WSHP stops when the temperature of the storage tank falls below 5°C to prevent the formation of ice. The parameters used in TRNSYS are shown in Table 1.

Table 1. System parameters used in TRNSYS modeling.

Model	Parameter	Value
Solar collectors	Intercept efficiency, $F_R(\tau\alpha)_{n'}$	0.8
(Type 1)	Efficiency slope, $F_R U_L$, W/(m²·K),	3.61
	Installation slope, degrees	40
Soil property parameters	Conductivity, W/(m·K)	1.5
(Type 707)[a]	Density, kg/m³	1500
	Specific heat, kJ/(kg·K)	2.2
	Convection coefficient, W/(m²·K)	17.78
Pump	Pump-1 (Solar pump) flow rate, kg/h	300
(Type 3b)	Pump-2 (Heating pump) flow rate, kg/h	100
	WSHP pump flow rate, kg/h	500
	Heating loop pump flow rate, kg/h	500
WSHP	Rated heat capacity, kW	30
(Type 225)	Rated COP	4
	Outlet water temp, °C	45
Building	Building capacitance, kJ/K	10000
(Type 88 with fan coil heating units	Building volume, m³/s	720
or Type12 c with floor heating system)	Initial temperature, °C	15
	Overall conductance of house, W/K	277.8
	Latent heat ratio	0.23
	Designed indoor temp, °C	20
	Initial humidity, g/kg (Type 88)	5
	Heat transfer rate of floor heating loop and the room, kJ/(h·K) (Type 12 c)	1200
	Building loss coefficient, kJ/(h·m²·K) (Type 12 c)	4.2
ASHP	Total air flow rate, 1/s	300.0
(Type 665–2)	Rated indoor fan power, kJ/h	671.1
	Rated outdoor fan power, kJ/h	745.7
Storage tank (Type 534)	Average tank loss coefficient, W/(m²·K)	0.33
	Initial storage temperature in all layers, °C	20
	Height-to-diameter ratio (HDR)	1
	Number of tank nodes	8
Pumps	Pump-1 (Solar pump) flow rate, kg/h	300
(Type 3b)	Pump-2 (Heating pump) flow rate, kg/h	100

[a]Data were taken from the reference (Zhang et al. 2006).

2.2.2. System B: ASHP heating system

The ASHP is very popular in this region. It is a cost-effective electricity-driven heating system that can also provide cooling in summer. Figure 3 shows a schematic of this system. In practice, System B could be a split air-conditioning unit or a variable refrigerant flow system. The parameters of the TRNSYS model of the system are shown in Table 1.

2.2.3. System C: ASHP + SWH

System C is an ASHP with the addition of an SWH as an additional heating source that works in parallel with the ASHP system. This SWH system has 40 m^2 flat plate solar collectors and a 2 m^3 tank for short-term storage of solar energy (Figure 4). The parameters of the TRNSYS model of the system are shown in Table 1.

The installation of the SWH for domestic hot water in urban buildings has been supported by government subsidies and has now become mandatory in most provinces in this region (He et al. 2015). However, the installation for space heating is still limited due to the high initial cost.
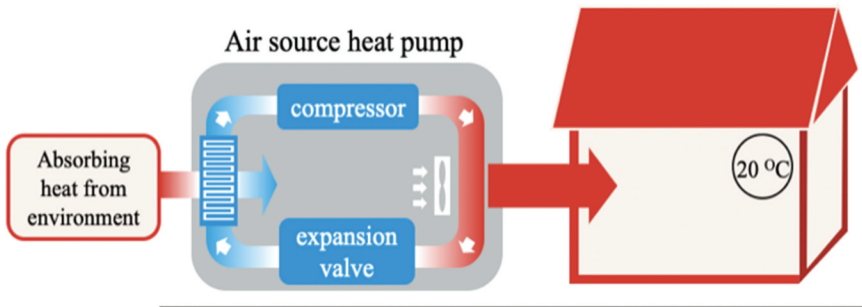

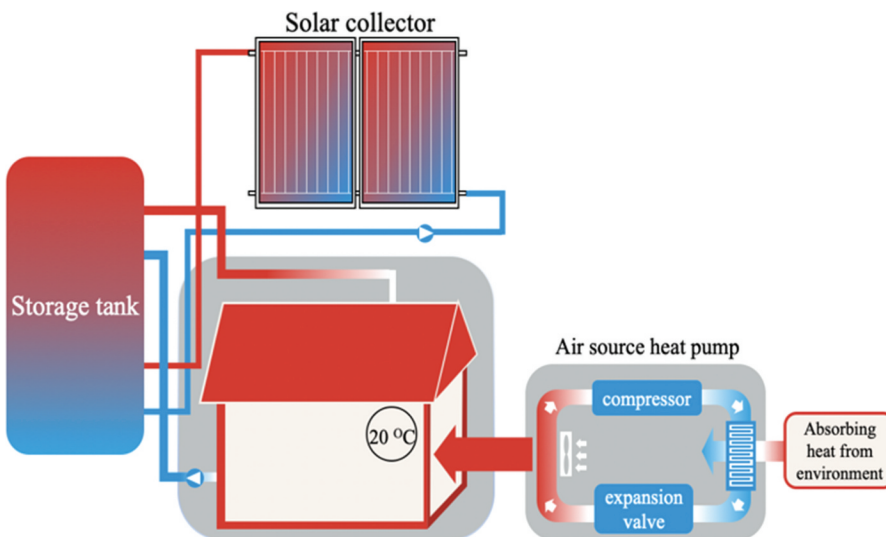**Figure 3.** System B: air-source heat pump (ASHP) with fan coil heating system.

Figure 4. System C: air-source heat pump (ASHP) with fan coil + solar water heater (SWH) for a floor heating system.

2.3. Economic analysis method

Both the net present value (NPV) (Hovsepian and Kaiser 1997; Martinopoulos and Tsalikis 2014) and the equivalent annual cost (EAC) (El-Bialy et al. 2016; Hirvonen, Ur Rehman, and Sirén 2018) have been used in the literature for economic analysis. The two values serve similar purposes. Both are based on a discount rate to evaluate an investment on an asset. The EAC is the annual cost of owning, operating, and maintaining an asset over its entire life. The NPV can be treated as the present value of owning and maintaining the heating system that generates an annuity equal to the amount of EAC during the lifespan. In this study, the EAC was selected (Equation (1)) because its meaning is more straightforward.

$$\text{EAC} = C \frac{i(1+i)^n}{(1+i)^n - 1} + P_E \times E + \alpha C \tag{1}$$

where C is the initial investment in Chinese Yuan (CNY), EAC is the equivalent annual cost of the system (CNY/y), i is the discount rate (interest rate or standard rate of return coefficient), n is the lifespan of the system (y), P_E is the electricity price (CNY/kWh), E is the total electrical demand (kWh), α is the ratio of the annual maintenance cost to the initial cost. The first term on the right is the average annual payment made to the bank for an initial loan amount of C. The remaining terms are associated with operating costs. Typically, plate type collectors have a lower rate of maintenance cost than vacuum collectors. In this study, α is 1%. The initial investment includes the equipment cost and installation of labor for all system components. In the STES system, the cost can be estimated using Equation (2).

$$C = P_C \times A + P_T \times V + C_{WSHP} + C_{P\&P} \tag{2}$$

where the subscript P&P stands for pumps and pipework. P_T is the cost of the storage tank (CNY/m^3), and P_C is the price of collectors (CNY/m^2). The determination of these values is shown in Table 2.

The high initial investment is attributable to the solar collector and the storage tank. The current average price of collectors is P_C = 1000 CNY/m^2 for flat plate types in China, including pump and pipework (Li et al. 2018; Orosz et al. 2016; Sonsaree et al. 2018). Experiences show that the unit cost can be reduced considerably for larger systems (Li and Zhu 2018; Orosz and Mathaha 2016; Sonsaree et al. 2018). In an earlier study, Pfeil and Koch (2000) compared the costs of two gravel/water thermal storage systems. They found that the cost of the more extensive system (16,000 m^3 water equivalent) was only one-third of the smaller system (1100 m^3 water equivalent). In this study, a unit cost of P_T = 1867 CNY/m^3 was estimated for a 40 m^3 underground cylinder-shaped concrete tank (Figure 5) with itemized costs listed in Table 3 based on current market values of labor and materials in China. For this type of storage tank, the reinforced concrete, stainless steel, insulation, and waterproof materials are the most expensive items. If the tank is a surface type, i.e., reinforced concrete is not used at the top regardless of burying, it may cost approximately 1,350 CNY/m^3. A plastic cylinder is much less expensive;

Table 2. Parameters used in the economic analysis (*1 CNY = 0.145188 USD).

	Symbol	Unit	Calculation
WSHP	C_{WSHP}	CNY	10,000
ASHP	C_{ASHP}	CNY	65,000
Pump and pipework	$C_{P\&P}$	CNY	3,000
Electricity price	P_E	CNY/kWh	0.518
Collector price	P_C	CNY/m^2	1,000
Tank price	P_T	CNY/m^3	1,867
Maintenance cost ratio	α	-	1%
Interest rate	i	-	8%

* Exchange ratio as of January 23, 2020, from China State Administration of Foreign Exchange is http://www.safe.gov.cn/safe/index.html
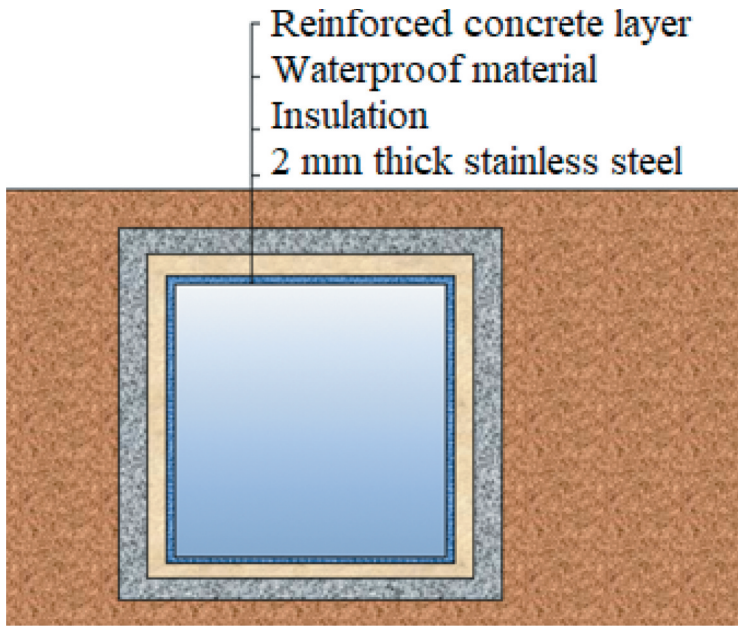
Figure 5. Schematic of an underground concrete water tank.

Table 3. Cost of an underground concrete tank (1 CNY = 0.145188 USD).

Composition	Cost (CNY)	Remark
Earth excavation	4,777	0.5 m soil on top
Backfilling soil	2,178	
Slab cushion	1,513	Bottom framework of reinforced concrete slab for leveling
Reinforced concrete wall	21,419	D = 3.7 m, L = 3.7 m
Insulation	9,777	75 mm Polyurethane
Waterproof material	10,429	Sprayed polyurea to prevent water intrusion
Interior lining	24,811	2 mm stainless steel plate
Total cost	74,903	

however, the market availability of low-cost plastic containers that can store up to 80°C to 90°C hot water cannot be ascertained. For large-scale storage systems, the unit cost of the storage system can be reduced significantly. For example, it was estimated to be 924 CNY/m^3 for a 5,274 m^3 tank constructed in the Jinke Heating and Power Plant in Inner Mongolia. In Heilongjiang province, a similar tank of 9,500 m^3 in the Huadian Fulaerji Electric Heating and Power Plant was constructed at the cost of approximately 800 CNY/m^3. Therefore, it can be assumed that the unit cost can be lower for a larger system.

3. Results and discussions

Energy performance is first discussed for the STES system with RVA = 40 m^3/40 m^2, followed by the optimization of the STES system with economic constraints.

3.1. Energy performance (RVA = 40 m^3/40 m^2)

Figure 6(a) plots the temporal variations of the total daily solar radiation and daily average collector efficiency. The collector efficiency is higher (40% to 60%) at the beginning of the charging period as
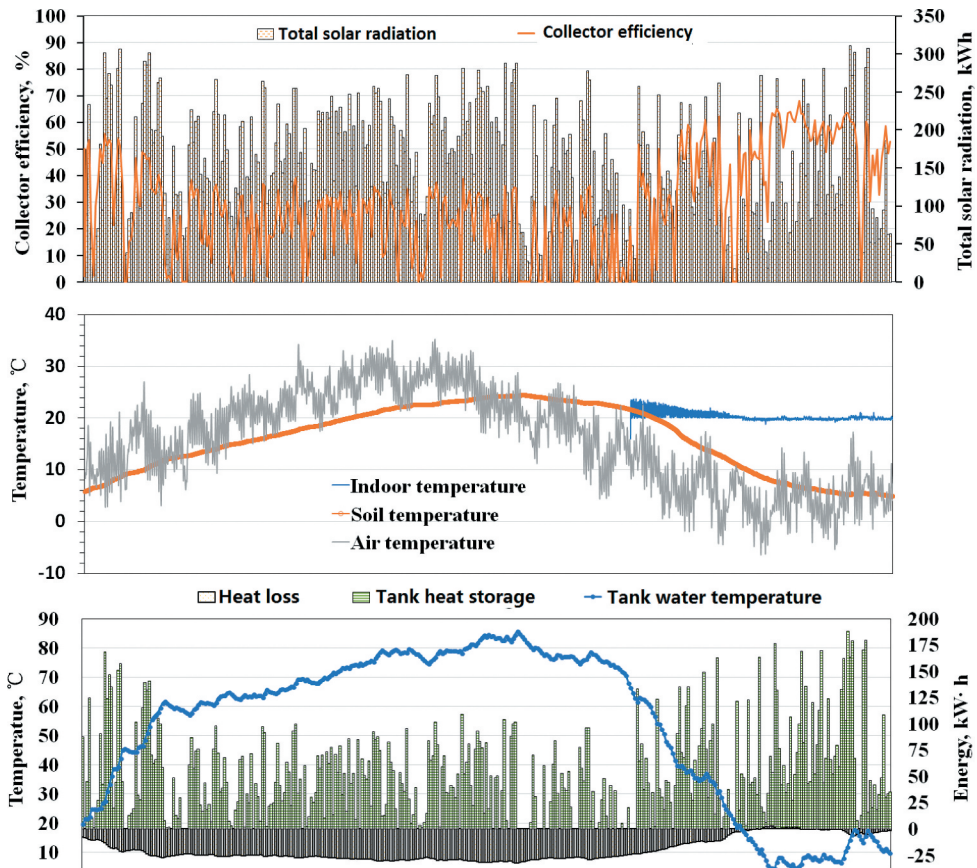
Figure 6. (a) Variation of the total daily solar radiation and daily average collector efficiency of the seasonal thermal energy storage (STES) system; (b) Simulated variation of annual indoor temperature along with soil and air temperatures; (c) Simulated water temperature in the tank.

well as in winter but is generally lower (<35%) during the summer and fall because of the increased water temperature in the storage tank. The magnitude of the collector efficiency matches that observed in actual projects (Jiao et al. 2015; Tao et al. 2015). Figure 6(b) shows that the dynamic indoor temperature was comfortable during the heating period, with an average of 20.4°C. At the beginning of the heating period, the indoor temperature fluctuates between the design value of 20°C and 23°C. Over-heating is a result of a constant speed pump. Figure 6(c) shows the variations of the average water temperature in the tank. The temperature increases at a relatively fast rate in the first month until it reaches about 60°C, after which it increases at a much slower rate. The reason is that, at high water temperatures, the collector efficiency drops quickly, and the heat loss of the tank increases. The water temperature continues to increase until it reaches the highest value of 86.2°C on September 26. Subsequently, it decreases due to relatively weaker solar radiation and lower ambient temperature. At the beginning of the heating period (November 15), the temperature of the tank is 70.8°C.

Direct heating can last for approximately 43 days until December 28 when the water temperature drops to 40°C. Thereafter, the WSHP is used to assist heating throughout the rest of the heating period in a serial mode of a solar-heat pump system where the tank temperature generally remains low.

Figure 7 shows the energy flow in the whole system. Approximately one-third, or 16,488 kWh, of the total incident solar energy is collected, almost half of which (7,035 kWh) is collected in winter. Approximately 45% of the collected energy is lost to the environment through pipe works, pumps, and soil contact. The solar fraction (ratio of the heating demand subtracted by the electricity demand to the
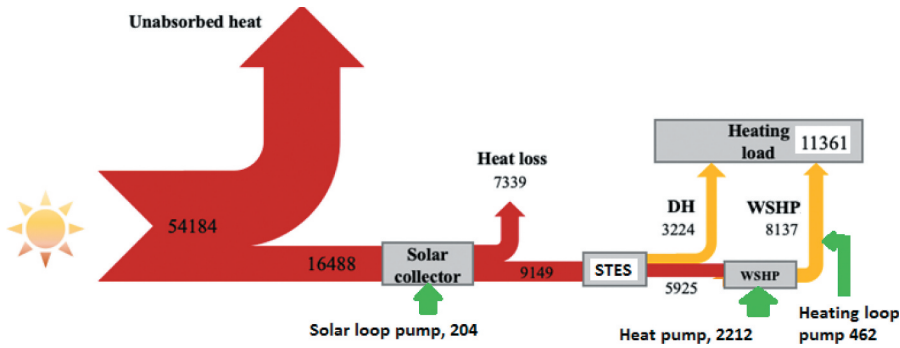
Figure 7. Energy flow in the seasonal thermal energy storage (STES)+solar water heating (SWH) system and electricity amounts (units: kWh).

heating demand) is 81%. The total electricity demand is 2,876 kWh and the system COP, the ratio of total heating demand to the total electricity demand, is 3.95. At a similar RVA, the storage efficiency (55%) and system COP are consistent with those of Li et al. (2014), and the solar fraction is consistent with that of Beausoleil-Morrison et al. (2019). According to Beausoleil-Morrison et al. (2019), increasing either the collector area or storage volume increases the solar fraction.

The energy performance of the three systems is compared in Figure 8. The COPs of systems B and C are 2.9 and 3.5, respectively; both are lower than that of system A. Compared with system B, system A reduces the electrical demand by approximately 40%. System C, which collects solar energy only in winter, reduces the electrical demand by approximately 14%. The STES increases the energy capacity of the collector (heating energy provided by collectors) from 51 kWh/m^2 in system C to 229 kWh/m^2 in system A, raising the solar fraction from 18% to 81%.

The calculated EAC costs are 9,861 CNY, 14,381 CNY, and 15,493 CNY for systems B, C, and A, respectively, assuming a lifetime of 20 y for all systems. As expected, the ASHP is the most economical
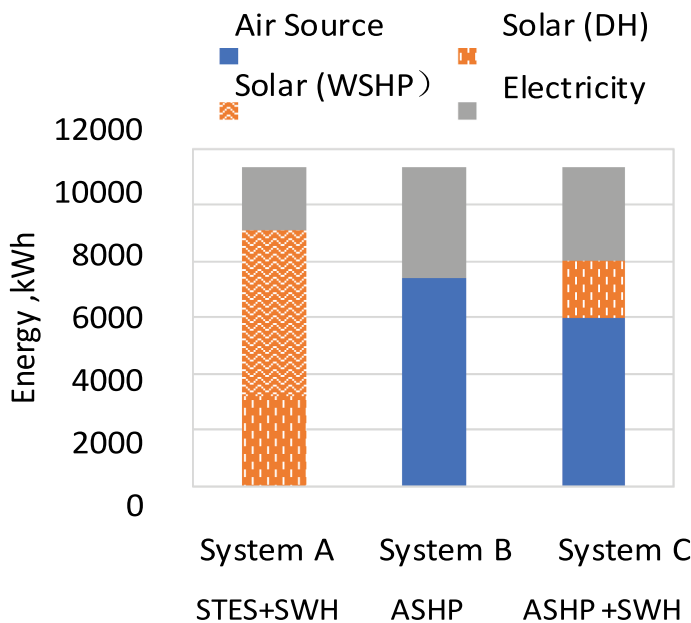

Figure 8. Comparisons of the energy performance of three systems (STES = seasonal thermal energy storage; SWH = solar water heater; ASHP = air-source heat pump).

solution, and adding a solar component solely for a winter application increases the cost by approximately 46%. Further addition of the seasonal storage system increases the annual cost further by 7.7%. The loan interest appears to be the largest share in the annual cost. Comparing system A with system B, the savings in energy cost, approximately 1,457 CNY/y, is far less than the increased annual cost in paying off the loan interest (4,780 CNY/y). Note that a discount interest rate is not considered here, although, in the literature, a discounted rate of 3% was adopted in the economic analyses (Hirvonen, Ur Rehman, and Sirén 2018; Renaldi and Friedrich 2019). If the loan interest i and the maintenance cost α are both zero, the EAC of system B (5,841 CNY/y) still remains significantly lower than that of system A (7,369 CNY/y) or system B (7,658 CNY/y). This analysis indicates that the current high prices of storage and collectors are the main factors preventing the STES system from competing against the ASHP system.

3.2. Optimized RVA values for the lowest annual cost

The optimal RVA value for the lowest annual cost was found with the constraint that the STES + WSHP system provides 100% of the heating demand. For any given tank volume, the minimum collector area that meets this constraint can be determined. Figure 9 shows the line of the minimum area along with the corresponding energy consumption and annual cost. As the line of the area moves to the left, the system has a smaller storage tank but a large collector area, approaching that of system C. As the line moves to the right, the system has a larger storage tank but a smaller collector area, applying more weight on the solar energy from the non-heating season. The most economical choice of sizes occurs at $A = 66$ m^2 and $V = 20$ m^3, or RVA = 0.3 m^3/m^2. The corresponding annual cost is 13,360 CNY/y, a reduction of 14% compared with the original design. The corresponding electrical demand is 1,269 kWh, reflecting 74% energy reduction compared with the ASHP system. Note that further energy-savings can be achieved if the collector area is increased; however, the cost will also increase.

The optimized RVA based on economic performance is considerably lower than those based on energy performance for large district heating systems (Dahash et al. 2019) but close to those suggested for small systems (Li et al. 2014; Ma et al. 2018). In a study by Durão et al. (2014) in Portugal, the
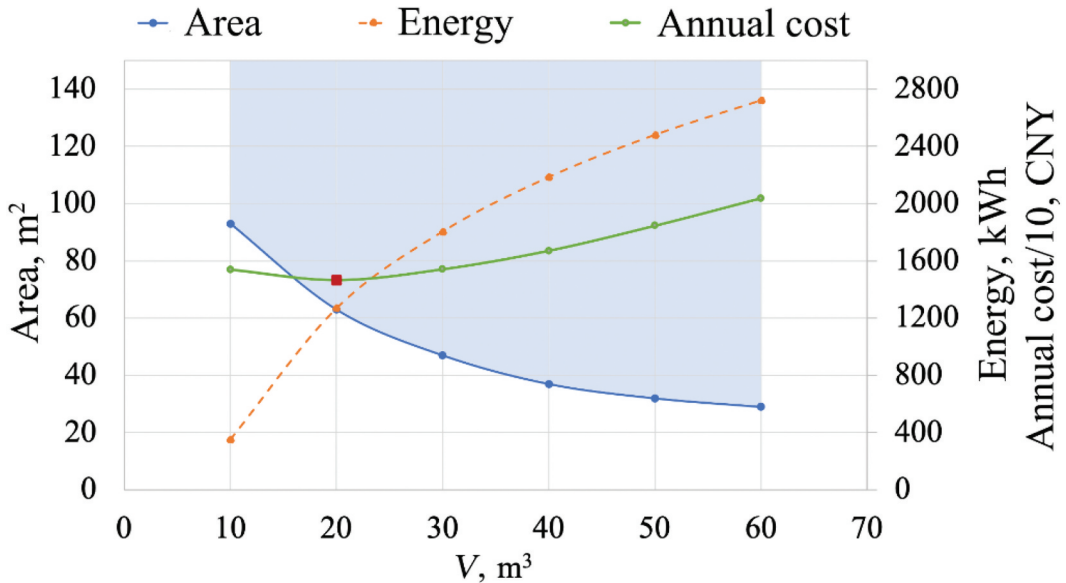

Figure 9. Minimum collector areas for given tank volumes to meet the heating demand plotted with the corresponding electrical demand and the equivalent annual cost.

optimal RVA value for the lowest annual cost was calculated to be 4.8 m^3/m^2 (1630/339) when the STES met 100% of the heating demand. However, the authors did not provide the market parameters used in their model. Milewski () recommended an RVA value of 0.7 m^3/m^2 for a reduced size system with a solar fraction of 53% after considering the total affordable initial cost rather than considering energy-saving returns. The smaller optimized RVA value in our study confirms the fact that seasonal storage is still an expensive technology for small-to-medium-sized STES systems in China.

3.3. Effect of market variables

Three market variables were examined for their influence on the economic performance of the STES: the tank price, collector price, and utility price. Figures 10 and 11 show the payback periods for replacing systems B and C with system A at different tank prices. Note that the line of P_E = 0.538 CNY/kWh and P_C = 1000 CNY/m^2 does not interact with the line P_T = 1867 CNY/m^3, implying that replacing system B with system A can never be profitable. This result is expected, considering that the STES is not even an economical choice compared with a conventional heating source such as natural gas or electricity (McKenna, Fehrenbach, and Merkel 2019). Here the ASHP is an efficient and mature market product.

Figures 10 and 11 show that the payback period decreases when the tank price or collector price decreases or the utility price increases. For the STES system to be profitable in practice, the payback period should be no more than the lifetime of the system (n_0 < 20 y). The threshold values (at n_0 = 20 y) of the three market prices are P_E = 2.5 CNY/y, P_T = 700 CNY/m^2, and P_C = −166 CNY/m^2. Independently, the practical applicability of these thresholds does not appear to be realizable soon for small systems as the values largely deviate from the current market values. The negative threshold value of the collector price implies that payback for the investment will be impossible, considering
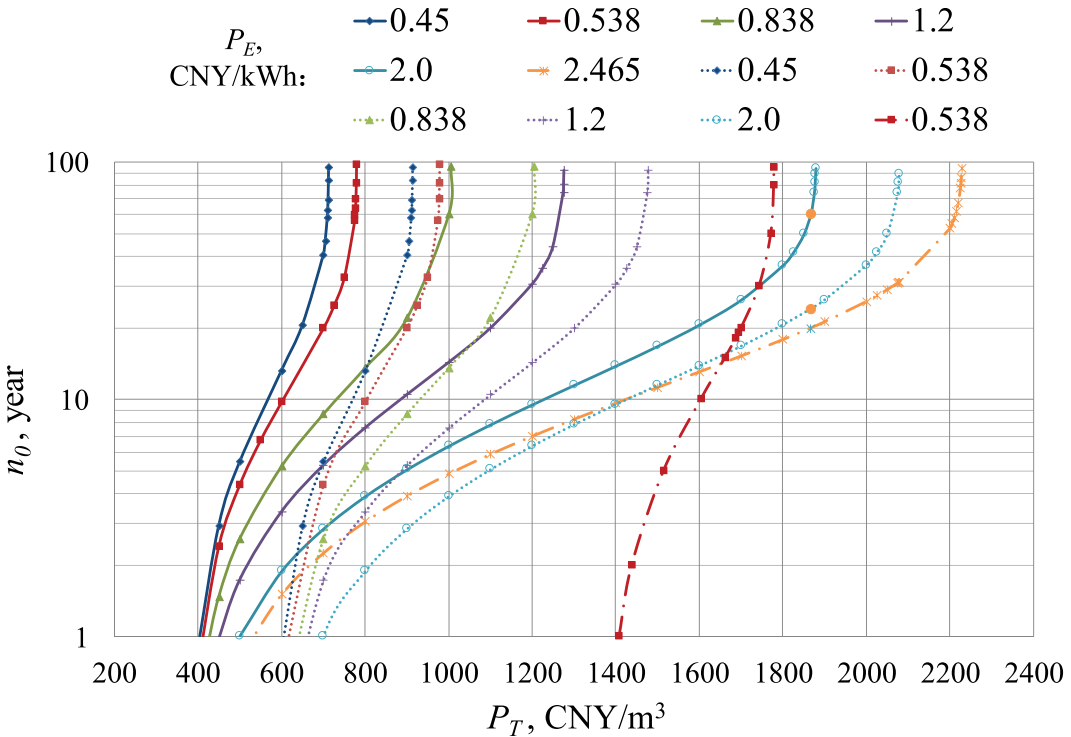

Figure 10. Payback periods of system A replacing system B under different market conditions. Solid lines: P_C = 1000 CNY/m^2; Dot lines: P_C = 800 CNY/m^2; Dash dot lines: P_C = 1.0 CNY/m^2.
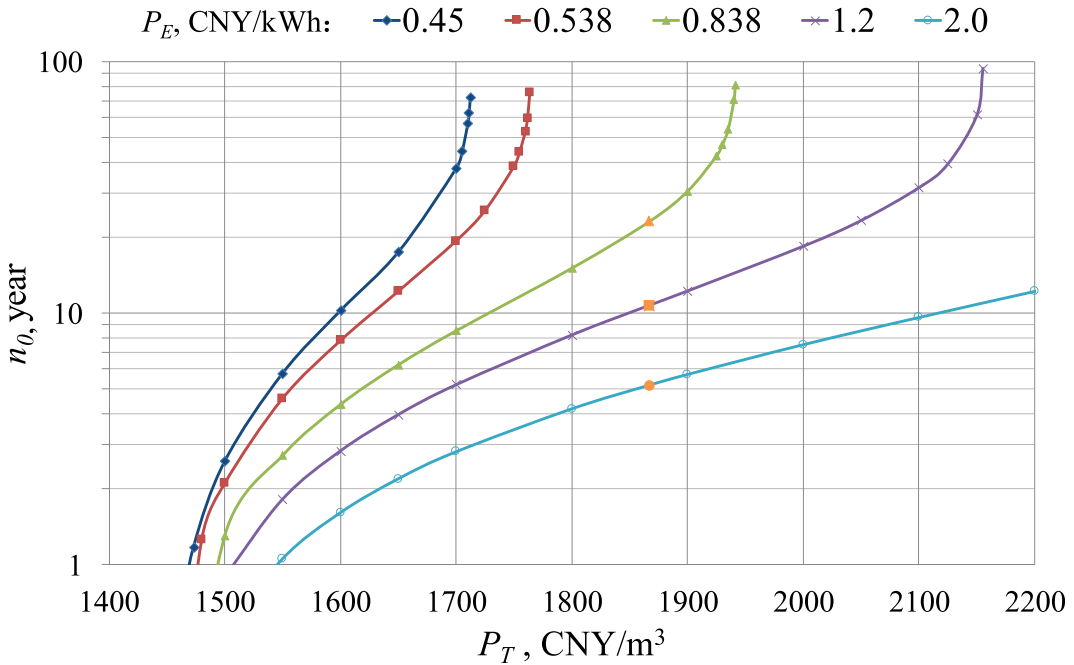
Figure 11. Payback periods of system A replacing system C (right) under different market conditions.

current tank prices and utility energy prices. A combination, however, is more practical. For example, the payback period can be reduced to 10 y at $P_E = 1.2$ CNY/kWh, $P_T = 1100$ CNY/m^2, and $P_C = 800$ CNY/m^2, which is a more practical combination through incentives. Note that the threshold $P_T = 700$ CNY/m^2 may be realizable for large storage tanks, as discussed in section 2.3, suggesting that the large-scale STES system for district heating projects may be already market-ready. This situation confirms some of the existing studies that predicted the market entry of district-scale STES systems in 2020 (IEA 2015; McKenna, Fehrenbach, and Merkel 2019).

Replacing system C with system A becomes economically advantageous either when the utility price reaches $P_E = 0.838$ CNY/kWh or when the tank price drops below $P_T = 1700$ CNY/m^3. Both values are practical. In fact, in Hangzhou, the residential utility price is 0.838 CNY/kWh after 4,800 kWh within the year. For the storage tank, such a price is realizable. Therefore, the current policy supporting SWH should shift toward supporting the installations of both collectors and the seasonal storage system.

The effect of market variables on the optimal RVA value for best economic performance is shown in Figure 12. The optimal ratio increases as the tank price decreases, as the utility price decreases, or as the collector price increases. In building integrated systems, a high RVA value is favorable because space is limited, and larger storage volume will have a larger solar fraction (Beausoleil-Morrison et al. 2019). The ratio is sensitive to the price of the tank and the collector, and, to a lesser extent, the utility price. For example, under current market conditions, the ratio would increase to 0.7 m^3/m^2 if the tank price declines to 1000 CNY/m^3. This ratio is in the range of medium-to-large-scale systems suitable for space heating for a large building complex or a community. Figure 12 can be used as a guideline for the design of the STES+SWH system in Hangzhou or other cities with similar solar resources.

3.4. Effect of interest rate

The interest rate depends on the country and the availability of incentives. A relatively wide range of interest rates has been used in the literature. Interest rates from 1.71% in Turkey (Martinopoulos and
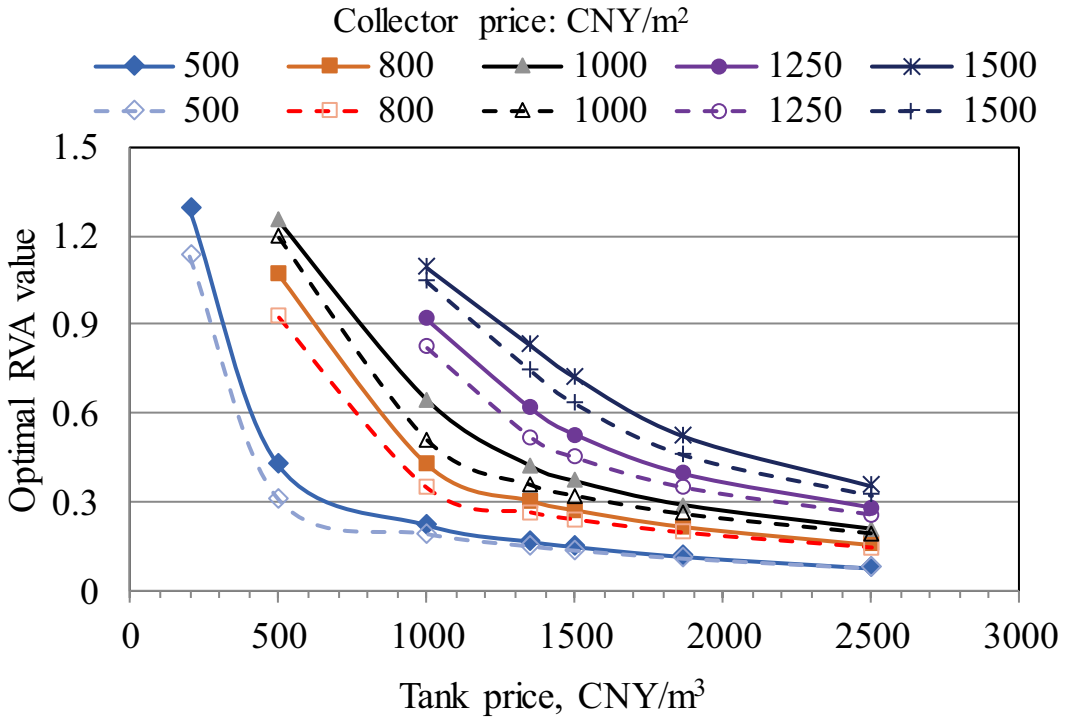
Figure 12. Effects of the tank price, collector price, and utility price on the variation of the optimal RVA value for the STES+SWH system (system A). Solid lines: P_E = 0.538 CNY/kWh; Dashed lines: P_E = 0.838 CNY/kWh.

Tsalikis 2014) to 12% in Egypt or Saudi Arabia (El-Bialy et al. 2016) have been reported. In the EU, 3% has been used (Hirvonen, Ur Rehman, and Sirén 2018).

In this studied case, the influence of interest rates on the EAC of the three systems is shown in Figure 13. Although the EAC in general decreases as the interest rate decreases, the decreasing rate is faster for more expensive systems. With a zero-interest rate, system A has the same annual cost as system C, indicating that the energy-savings from the seasonal storage system balance the increased investment cost within the lifetime of the system. The figure also shows that system A still cannot compete against system B in the market if the discounted interest rate is the only incentive measure. However, if the construction cost of the tank can be reduced to 800 CNY/m^3, the EAC of system A becomes lower than that of system B once the interest rate is less than 3%, confirming the previous finding that large STES systems may be market competitive.

3.5. Effect of the storage period

For systems with a smaller RVA value, it is tempting to shorten the collecting period as there is more energy in the non-heating season than can be stored. It was discovered that the solar collecting period can be reduced without sacrificing the amount of heating energy delivered. As shown in Figure 14, the best energy efficiency is achieved when the starting date for charging is postponed until July 17. Similar results can be found in (Li et al. 2015), where the best starting time was found to be May 1 instead of March 15, the end of the heating season, for the optimization of STES system. However, in this study, the total energy-savings by postponing the starting date is small: 45 kWh, or a 2% reduction in the overall energy demand. The reason is that the pumping energy of the solar loop has a small share in the total electrical demand.
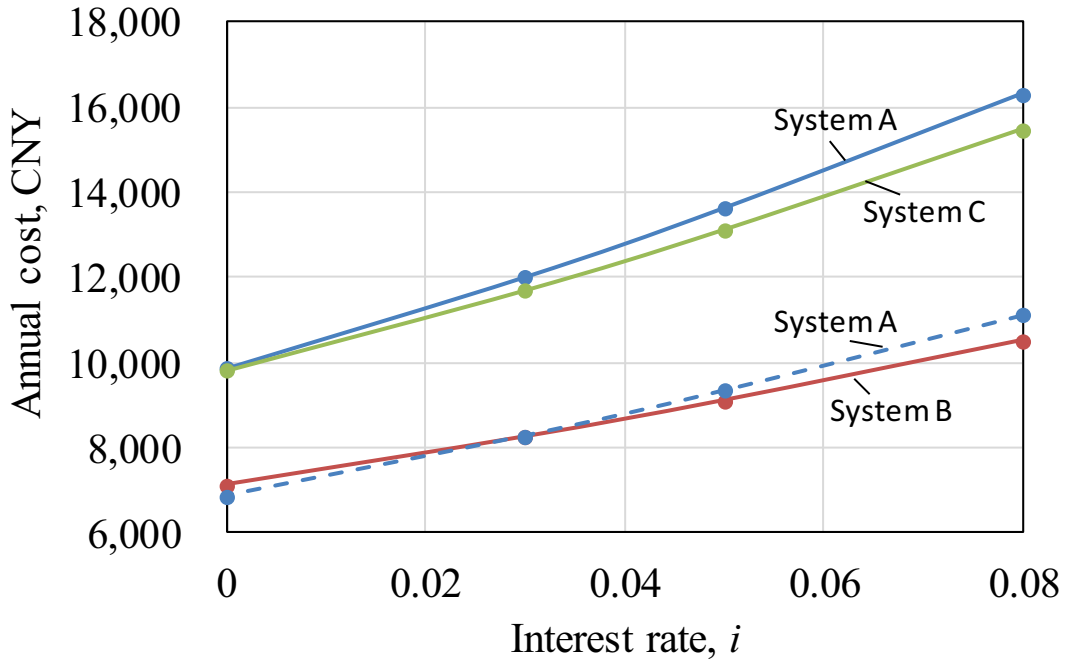
Figure 13. Effect of interest rate on the annual cost of three systems. Solid lines: current market conditions; Dashed lines: current market condition except for P_T = 800 CNY/m³.

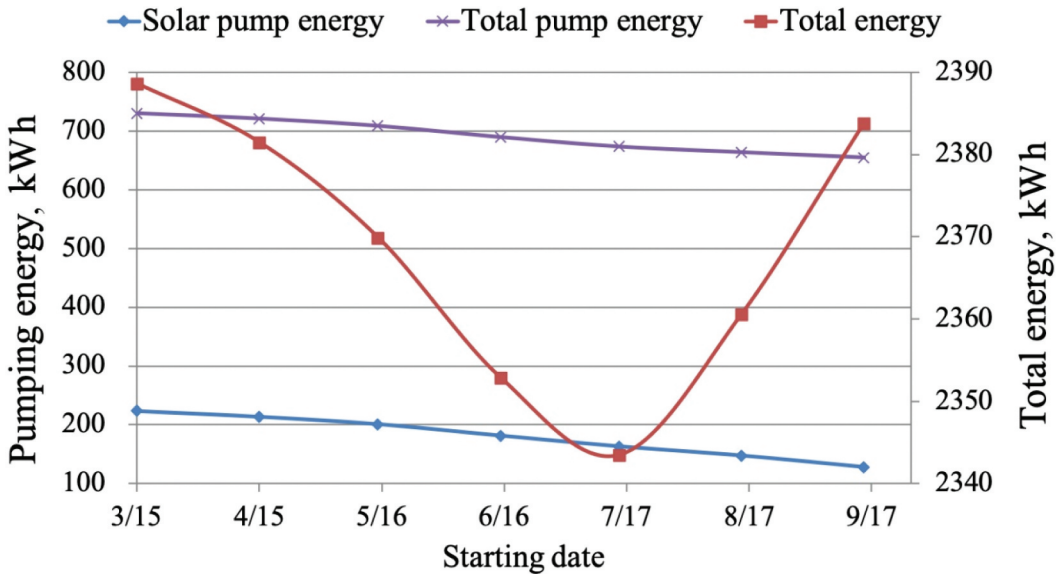**Figure 14.** Relationship between the starting date of seasonal storage and the total electricity demand.

4. Conclusions

This study evaluated the techno-economics of replacing the ASHP system with the STES system for residential space heating under the climatic conditions of Hangzhou city in China. Simulation in TRNSYS showed that the STES with an RVA = 40/40 m³/m² achieves a solar fraction of 81% and an

overall system COP of 3.95. Compared with the ASHP system, the STES achieves 40% energy-saving. Compared with conventional solar heating system, the STES could increase the energy capacity of collectors from 51 to 229 kWh/m^2.

The RVA of the STES system was optimized using the EAC method, and the sensitivity of market variables was analyzed. The most economic RVA was found to be 0.33 m^3/m^2 under current market conditions for the studied case. This RVA corresponds to 66 m^2 of collector area, and 20 m^3 of tank volume. The electricity demand was 1,269 kWh, reflecting 74% of the energy-saving compared with the ASHP heating system. Sensitivity analysis showed that the RVA is sensitive to market prices. The ratio increases when the tank price increases or when the collector price decreases or when the utility price is higher.

Despite the considerable energy performance of the STES over the ASHP system or conventional solar-assisted ASHP system, its replacement of the ASHP system for space heating is not economical at current market prices of electricity, tank storage, and collectors. For the STES to be market competitive, the threshold prices for electricity and the storage tank were calculated to be 2.5 CNY/kWh and 700 CNY/m^3, respectively. Large STES systems may already be market-ready because of the reduction of storage tank price. For small systems, policy support is required. Reduction in the collector price or the interest rate alone cannot achieve a realizable payback period; however, it could play a role in a combination of policy measures that aim to achieve the above price thresholds. For heating systems already designed with solar collectors, the addition of STES is economically beneficial considering current market conditions.

In addition to the effort of reducing unit prices of tanks, collectors, and electricity, reducing the physical size of the storage system while maintaining the same storage capacity is desirable for residential application. The breakthrough may lie in new materials and technologies associated with high energy storage density, such as the adsorption storage technology (Xu and Wang 2019). Finally, our analysis does not consider the greater demand flexibility offered by the seasonal energy storage. In the future, the quantification of demand flexibility (Stavrakas and Flamos 2020) and its associated economic and social benefits could be taken into account.

ORCID

Guoqing He (iD) http://orcid.org/0000-0002-7667-2335

References

Antoniadis, C. N., and G. Martinopoulos. 2019. Optimization of a building integrated solar thermal system with seasonal storage using TRNSYS. *Renewable Energy* 137:56–66. doi:10.1016/j.renene.2018.03.074.

Azeez, N. T., and U. Atikol. 2019. Utilizing demand-side management as tool for promoting solar water heaters in countries where electricity is highly subsidized. *Energy Sources, Part B: Economics, Planning, and Policy* 14 (2):34–48. doi:10.1080/15567249.2019.1595224.

Beausoleil-Morrison, I., B. Kemery, A. D. Wills, and C. Meister. 2019. Design and simulated performance of a solar-thermal system employing seasonal storage for providing the majority of space heating and domestic hot water heating needs to a single-family house in a cold climate. *Solar Energy* 191:57–69.100. doi:10.1016/j. solener.2019.08.034.

Bokhoven, T., and J. Van Dam. 2001. Recent experience with large solar thermal systems in the Netherlands. *Solar Energy* 71 (5):347–52. doi:10.1016/S0038-092X(00)00124-9.

China Meteorological Administration, Tsinghua University. 2005. *Meteorological data set for China building thermal environment analysis*. Beijing: China Architecture and Building Press.

Chung, M., J. U. Park, and H. K. Yoon. 1998. Simulation of a central solar heating system with seasonal storage in Korea. *Solar Energy* 64 (4):163–78. doi:10.1016/S0038-092X(98)00101-7.

Dahash, A., F. Ochs, M. B. Janetti, W. Streicher. 2019. Advances in seasonal thermal energy storage for solar district heating applications: A critical review on large-scale hot-water tank and pit thermal energy storage systems. *Applied Energy* 239:296–315. doi:10.1016/j.apenergy.2019.01.189.

Durão, B., A. Joyce, J. F. Mendes. 2014. Optimization of a seasonal storage solar system using Genetic Algorithms. *Solar Energy* 101:160–66. doi:10.1016/j.solener.2013.12.031.

El-Bialy, E., S. M. Shalaby, A. E. Kabeel, A. M. Fathy. 2016. Cost analysis for several solar desalination systems. *Desalination* 384:12–30. doi:10.1016/j.desal.2016.01.028.

Fatih Demirbas, M. 2006. Thermal energy storage and phase change materials: An overview. *Energy Sources, Part B: Economics, Planning and Policy* 1 (1):85–95. doi:10.1080/009083190881481.

Guadalfajara, M., M. A. Lozano, L. M. Serra. 2015. Simple calculation tool for central solar heating plants with seasonal storage. *Solar Energy* 120:72–86. doi:10.1016/j.solener.2015.06.011.

Hang, Y., M. Qu, and F. Zhao. 2012. Economic and environmental life cycle analysis of solar hot water systems in the United States. *Energy and Buildings* 45:181–88. doi:10.1016/j.enbuild.2011.10.057.

He, G., Y. Zheng, Y. Wu, Z. Cui, K. Qian. 2015. Promotion of building-integrated solar water heaters in urbanized areas in China: Experience, potential, and recommendations. *Renewable and Sustainable Energy Reviews* 42:643–56. doi:10.1016/j.rser.2014.10.044.

Hepbasli, A., K. Ulgen, and R. Eke. 2004. Solar energy applications in Turkey. *Energy Sources* 26 (6):11. doi:10.1080/00908310490438579.

Hesaraki, A., A. Halilovic, S. Holmberg. 2015. Low-temperature heat emission combined with seasonal thermal storage and heat pump. *Solar Energy* 119:122–33. doi:10.1016/j.solener.2015.06.046.

Hirvonen, J., H. Ur Rehman, K. Sirén. 2018. Techno-economic optimization and analysis of a high latitude solar district heating system with seasonal storage, considering different community sizes. *Solar Energy* 162:472–88. doi:10.1016/j.solener.2018.01.052.

Hovsepian, A., and M. Kaiser. 1997. Economics of installation of an active solar heating system. *Energy Sources* 19 (2):163–72. doi:10.1080/00908319708908841.

Huang, H., and H. Huang. 2017. Chinas policies and plans for clean energy production. *Energy Sources, Part B: Economics, Planning and Policy* 12 (12):1046–53. doi:10.1080/15567249.2017.1349214.

Huang, J., J. Fan, and S. Furbo. 2019. Feasibility study on solar district heating in China. *Renewable and Sustainable Energy Reviews* 108:53–64. doi:10.1016/j.rser.2019.03.014.

IEA. 2015. Seasonal thermal energy storage: Report on the state of the art and necessary further R&D solar heating and cooling programme, Task 45 large systems, L. D. E. Dirk Mangold. Solites Stuttgart.

Jiao, Q., W. Liu, G. Liu, Y. Zhang, J. Cai, H. Qin. 2015. Data measurement and analysis of a solar heating system with seasonal storage. *Energy Procedia* 70:241–48. doi:10.1016/j.egypro.2015.02.120.

Jradi, M., C. Veje, B. N. Jørgensen. 2017. Performance analysis of a soil-based thermal energy storage system using solar-driven air-source heat pump for Danish buildings sector. *Applied Thermal Engineering* 114:360–73. doi:10.1016/j.applthermaleng.2016.12.005.

Klein, S., W. Beckmanl. 2004. *TRNSYS 16–a transient system simulation program, user manual, Madison*. University of Wisconsin-Madison: Solar Energy Laboratory.

Krupczak, J. J., P. Skilman, A. Brancic, and J. E. Sunderland. 1986. Seasonal storage of solar energy using insulated earth. In *INTERSOL85: Proceedings of the Ninth Biennial Congress of the International Solar Energy Society*, ed. E. Bilgen and K. G. T. Hollands, 806–10. Oxford: Pergamon.

Launay, S., B. Kadoch, O. Le Métayer, and C. Parrado. 2019. Analysis strategy for multi-criteria optimization: Application to inter-seasonal solar heat storage for residential building needs. *Energy* 171:419–34. doi:10.1016/j.energy.2018.12.181.

Leckner, M., and R. Zmeureanu. 2011. Life cycle cost and energy analysis of a net zero energy house with solar combisystem. *Applied Energy* 88 (1):232–41. doi:10.1016/j.apenergy.2010.07.031.

Li, H., L. Sun, Y. Zhang. 2014. Performance investigation of a combined solar thermal heat pump heating system. *Applied Thermal Engineering* 71 (1):460–68. doi:10.1016/j.applthermaleng.2014.07.012.

Li, J., C. Zhu. 2018. Economic analysis of solar powered absorption refrigeration system powered by different solar collectors. *Advances in New and Renewable Energy* 6 (5):379–86. doi:10.1016/j.renene.2017.11.055.

Li, T., Y. Liu, D. Wang, K. Shang, and J. Liu. 2015. Optimization analysis on storage tank volume in solar heating system. *Procedia Engineering* 121:1356–64. doi:10.1016/j.proeng.2015.09.019.

Li, Y. W., R. Z. Wang, J. Y. Wu, and X. Xu. 2007. Experimental performance analysis on a direct-expansion solar-assisted heat pump water heater. *Applied Thermal Engineering* 27 (17–18):2858–68. doi:10.1016/j.applthermaleng.2006.08.007.

Liu, Y., J. Ma, G. Zhou, C. Zhang, W. Wan. 2016. Performance of a solar air composite heat source heat pump system. *Renewable Energy* 87:1053–58. doi:10.1016/j.renene.2015.09.001.

Ma, Z., H. Bao, A. P. Roskilly. 2018. Feasibility study of seasonal solar thermal energy storage in domestic dwellings in the UK. *Solar Energy* 162:489–99. doi:10.1016/j.solener.2018.01.013.

Marcos, J. D., M. Izquierdo, and D. Parra. 2011. Solar space heating and cooling for Spanish housing: Potential energy savings and emissions reduction. *Solar Energy* 85 (11):2622–41. doi:10.1016/j.solener.2011.08.006.

Martinopoulos, G., and G. Tsalikis. 2014. Active solar heating systems for energy efficient buildings in Greece: A technical economic and environmental evaluation. *Energy and Buildings* 68:130–37. doi:10.1016/j.enbuild.2013.09.024.

Martinopoulos, G., and G. Tsalikis. 2018. Diffusion and adoption of solar energy conversion systems – the case of Greece. *Energy* 144:800–07. doi:10.1016/j.energy.2017.12.093.

McKenna, R., D. Fehrenbach, and E. Merkel. 2019. The role of seasonal thermal energy storage in increasing renewable heating shares: A techno-economic analysis for a typical residential district. *Energy and Buildings* 187:38–49. doi:10.1016/j.enbuild.2019.01.044.

Milewski, J., M. Wołowicz, and W. Bujalski. 2013. Seasonal thermal energy storage - a size selection. *Applied Mechanics and Materials* 467:270–76. doi:10.4028/www.scientific.net/AMM.467.270.

Ochs, F., W. Heidemann, H. Müller-Steinhagen. 2009. Performance of large-scale seasonal thermal energy stores. *Journal of Solar Energy Engineering* 131 (4):041005–1–041005–5. doi:10.1115/1.3197842.

Orosz, M., P. Mathaha. 2016. Low-cost small scale parabolic trough collector design for manufacturing and deployment in Africa. *AIP Conference Proceedings* 1734:020016.

Paksoy, H., O. Andersson, S. Abaci, H. Evliya, B. Turgut. 2000. Heating and cooling of a hospital using solar energy coupled with seasonal thermal energy storage in an aquifer. *Renewable Energy* 19 (1–2):117–22. doi:10.1016/S0960-1481(99)00060-9.

Pfeil, M., and H. Koch. 2000. High performance-low cost seasonal gravel water storage pit. *Solar Energy* 69 (6):7. doi:10.1016/S0038-092X(00)00123-7.

Renaldi, R., and D. Friedrich. 2019. Techno-economic analysis of a solar district heating system with seasonal thermal storage in the UK. *Applied Energy* 236:388–400. doi:10.1016/j.apenergy.2018.11.030.

Shah, S. K., L. Aye, B. Rismanchi. 2018. Seasonal thermal energy storage system for cold climate zones: A review of recent developments. *Renewable and Sustainable Energy Reviews* 97:38–49. doi:10.1016/j.rser.2018.08.025.

Sonsaree, S., T. Asaoka, S. Jiajitsawat, H. Aguirre, K. Tanaka. 2018. A small-scale solar organic rankine cycle power plant in Thailand: Three types of non-concentrating solar collectors. *Solar Energy* 162:541–60. doi:10.1016/j.solener.2018.01.038.

Sovacool, B. K., and M. Martiskainen. 2020. Hot transformations: Governing rapid and deep household heating transitions in China, Denmark, Finland and the United Kingdom. *Energy Policy* 139:111330. doi:10.1016/j.enpol.2020.111330.

Stavrakas, V., and A. Flamos. 2020. A modular high-resolution demand-side management model to quantify benefits of demand-flexibility in the residential sector. *Energy Conversion and Management* 205:112339. doi:10.1016/j.enconman.2019.112339.

Sweet, M. L., and J. T. McLeskey. 2012. Numerical simulation of underground seasonal solar thermal energy storage (SSTES) for a single family dwelling using TRNSYS. *Solar Energy* 86 (1):289–300. doi:10.1016/j.solener.2011.10.002.

Tao, T., F. Zhang, W. Zhang, P. Wan, X. Shen, H. Li. 2015. Low cost and marketable operational experiences for a solar heating system with seasonal thermal energy storage (SHSSTES) in Hebei (China). *Energy Procedia* 70:267–74. doi:10.1016/j.egypro.2015.02.123.

Urmeea, T., E. Walker, P. A. Bahri, G. Baverstock, S. Rezvani, and W. Saman. 2018. Solar water heaters uptake in Australia – Issues and barriers. *Sustainable Energy Technologies and Assessments* 30:13.

Walton, M., and P. McSwiggen. 1983. Heat accumulation, storage and recovery in flooded mines at Ely, Minnesota, US. International Conference on Subsurface Heat Storage in Theory and Practice, Stockholm, Sweden, June 6–8.

Xu, Z. Y., and R. Z. Wang. 2019. Absorption seasonal thermal storage cycle with high energy storage density through multi-stage output. *Energy* 167:1086–96. doi:10.1016/j.energy.2018.11.072.

Zhang, D., J. Zheng, F. Huang. 2014. Investigation and analysis of heating in hot summer and cold winter zone. *HV& AC (Chinese)* 44 (6):21–24.

Zhang, L., P. Xu, J. Mao, X. Tang, Z. Li, and J. Shi. 2015. A low cost seasonal solar soil heat storage system for greenhouse heating: Design and pilot study. *Applied Energy* 156:213–22. doi:10.1016/j.apenergy.2015.07.036.

Zhang, M., M. Wang, J. Fu. 2006. *Urban soil research in Hangzhou*. Beijing, China: China Agricultural Science and Technology Press.

Zhou, Z., C. Wang, X. Sun, F. Gao, W. Feng, and G. Zillante. 2018. Heating energy saving potential from building envelope design and operation optimization in residential buildings: A case study in northern China. *Journal of Cleaner Production* 174:413–23. doi:10.1016/j.jclepro.2017.10.237.